Advanced Review

High efficiency photovoltaics: on the way to becoming a major electricity source

Xiaoting Wang,[1] John Byrne,[1]* Lado Kurdgelashvili[1] and Allen Barnett[2]

The dramatic growth of the photovoltaic (PV) industry—accelerated by increased economies of scale, technology improvements, research and development efforts, and strong policy support—has pushed PV to set out on its pathway to becoming a major electricity source. The speed and course of this pathway will be determined by the development of PV energy price and its relation to market electricity sales price. The current gap between PV energy price and market electricity sales is often covered by substantial government subsidies. Using the United States PV market as a case study to illustrate the need for PV energy price decline, this article details the potential contribution of high-efficiency PV based on different materials to realize such a decline and a substantial PV electricity share. It is found that—with considerable government support—PV's electricity share in the United States can rise to 25% by 2050. In order to help the PV industry achieve significant progress without large government subsidies, more radical decline of PV system cost is necessary. As such, quantitative analysis is deployed to investigate the value of module efficiency in lowering the total PV electricity cost through a levelized cost of energy analysis. Next, the article investigates in detail the research and development opportunities for high-efficiency PV and projects the required efficiency-price ranges for different types of PV modules.

How to cite this article:
WIREs Energy Environ 2012, 1: 132–151 doi: 10.1002/wene.44

INTRODUCTION

Half a century after the publication of Albert Einstein's technical paper explaining the photovoltaic (PV) effect, the first solar cell that was capable of generating enough power to run everyday electrical equipment was developed at Bell Laboratories in 1954.[1] By the end of the same century, world PV installations had developed to the order of 1 GW capacity.[2] During the past decade since 2002, the world cumulative PV capacity has increased from 2.26 to 67.4 GW,[2,3] with an average annual increase rate of 57.4% for new installations. Assuming annual electricity generation of 1500 kWh per kW PV, 101 billion kWh of electricity could have been provided by PV by the end of 2011, a corresponding 0.57% of the world electricity consumption in the same year.[4] Although still in the early stages of its development, PV has set out on the journey to becoming a serious electricity source.

Accompanying the dramatic increase of PV installations, PV system price experienced a remarkable decline. Figure 1 shows the price learning curve of the core component in a PV system, the module. The derivation is based on data from 1980 to 2010.[2,5] Although this achievement can to a great extent be attributed to the increased economies of scale, it has been benefiting significantly from constant progress of research and development (R&D). For comparison purpose, we also present the price data of the core component in a wind power system, the turbine, from 1996 to 2010.[2,6] Although the learning curve

*Correspondence to: jbbyrne@udel.edu

[1]Center for Energy and Environmental Policy, University of Delaware, Newark, DE, USA

[2]School of Photovoltaics and Renewable Energy Engineering, University of Delaware, Newark, DE, USA

DOI: 10.1002/wene.44

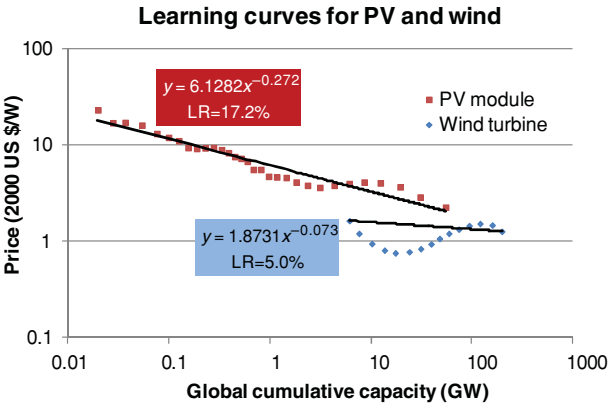

FIGURE 1 | Price learning curves for PV modules and wind turbines. The data on the *y*-axis for PV modules corresponds to global average price.[5] The data on the *y*-axis for wind turbines corresponds to the US case that demonstrated a good match with the worldwide case during the past 6 years.[6]

for PV module price is derived based on the normal least squares (NLSs) method with a good linearity under logarithmic scales, the learning curve for wind turbine price is simply based on the data for 1996 and 2010. This is because the learning curve derived with the NLS method demonstrates an increasing tendency as cumulative capacity increases due to the divergence of the price data. PV module price has a learning rate that is more than three times of that for wind turbine price. The great learning ratio for PV module price has greatly benefited from the deeper and wider exploration space, thanks to the rich R&D opportunities at multiple levels, including developments in material, solar cell structure, module structure, fabrication equipment, etc.

Currently, there still exists a gap between the price of PV generated electricity and the market electricity sales price, and this gap is compensated by the government in the form of subsidy. In this article, we use the PV market in the United States as a study case to illustrate the necessity for accelerating PV energy price decline, in order to realize PV as a major electricity source by the middle of this century, without strong dependence on government subsidy.

Because of the need for faster PV energy price decline, this article investigates the value of module efficiency in lowering the total PV electricity cost. Quantitative analysis is deployed based on the concept that a great portion of PV system cost is either fixed or related to installation area, and this part of cost can be reduced when modules of higher efficiency are adopted, leading to a lower PV energy cost.

Considering the contribution of high module efficiency in lowering PV energy cost, we then focus on R&D opportunities for high efficiency modules that are based on solar cells of different materials, including silicon (Si), Copper Indium Gallium Selenide (CIGS), cadmium telluride (CdTe), Gallium Arsenide (GaAs), and other III–V materials. These opportunities cover multiple levels of improvements, ranging from material quality, cell and module structures, and conditions that affect module efficiency in long-term operation.

At the end of this article, we briefly summarize the R&D opportunities and project the required efficiency–price ranges for different types of PV modules by setting a target PV energy cost of 10 ¢/kWh. Two projections are made based on current nonmodule costs and a 30% reduction of these costs. Under the assumption of a 30% cut on nonmodule costs, flat plate PV modules can be competitive with an efficiency range of 12–26% and the corresponding cost range of 0.9–1.6 $/W. Under the same assumption, concentrating PV modules can be competitive in the efficiency range of 30–40%, with the corresponding cost range of 1.0–1.2 $/W.

PV DIFFUSION IN THE UNITED STATES AND GRID PARITY PROJECTION

Since 1992, the cumulative capacity of PV installations in the United States has been increased from 43.5 MW to more than 3500 MW,[a,7,8] and PV generated electricity has achieved 0.1% of the total US electricity generation for the first time in 2011, assuming an annual electricity generation of 1500 kWh per kW PV. In this section, we analyze the market diffusion demonstrated by the history of PV installations, and we use this to benchmark future development.

Figure 2 depicts the cumulative PV installations in the United States from 1992 to 2011.[7,8] For convenient analysis, we present the same data in the semi-log coordinate system, as shown in Figure 3.

In Figure 3, we divide the data into two groups for a better fit to the exponential model. The greater slope for the trend line incorporating the second group of data reflects a more intense market penetration of PV technology in recent years. To predict the future diffusion, we adopt two models here. The first is the exponential model, as indicated by the trend line covering the more recent data in Figure 3 and

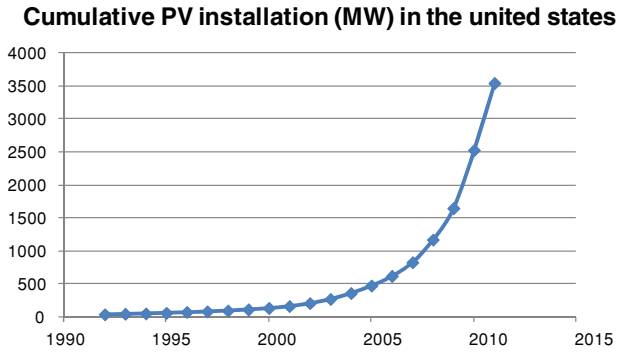

FIGURE 2 | Cumulative US PV installed capacity from 1992 to 2011,[7,8] presented in a linear coordinate system.

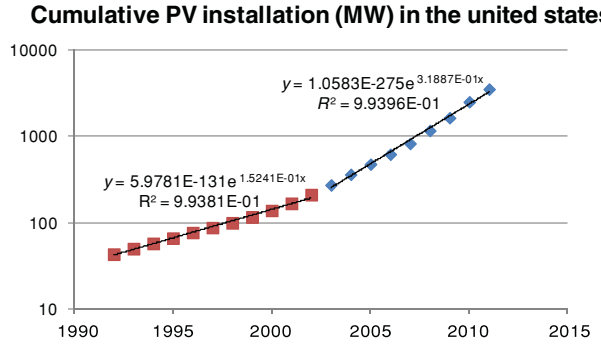

FIGURE 3 | Cumulative US PV installed capacity from 1992 to 2011,[7,8] presented in a semi-log coordinate system. Exponential growth pattern is assumed to derive two tendency lines.

expressed in Eq. (1):

$$Q_t = 1.0583E^{-275}e^{0.3189t} \tag{1}$$

where t and Q_t stand for the time (in years) and the cumulative PV installation corresponding to the time, respectively.

In the second method, we consider market saturation and adopt a logistic growth model.[9,10] The diffusion pattern under this model can be expressed as:

$$Q_t = \frac{U}{1 + e^{-b(t-t_m)}} \tag{2}$$

or

$$\ln\left(\frac{U - Q_t}{Q_t}\right) = -bt + bt_{\mathrm{m}} \tag{3}$$

where t and Q_t stand for the time (in years) and the ratio of PV generated electricity to the total electricity generation in the United States, corresponding to the time; U is the saturation level for Q_t; b is a slope term that reflects the initial growth rate; t_{m} is a time variable that represents the midpoint of the logistic curve.

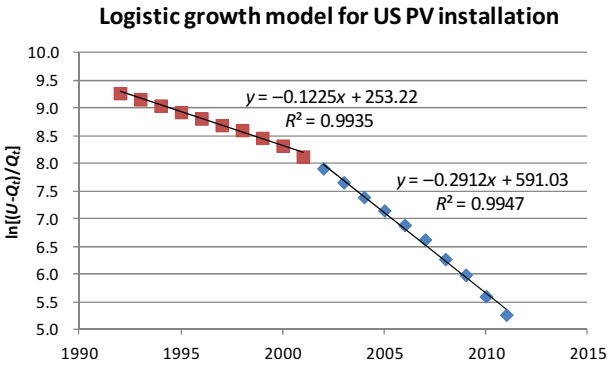

FIGURE 4 | Logistic growth model for US PV installation based on data from 1992 to 2011.[7,8,12,13]

For the logistic growth model, we set 25% as the saturation level for Q_t.[11] Assuming 1500 kWh as the annual electricity generation per kWh PV capacity and adopting the annual total electricity generation in the United States,[12,13] the value of Q_t can be calculated, as shown in Figure 3. Considering the data of more recent years (represented by the blue dots in Figure 4), Eq. (3) can be written as:

$$\ln\left(\frac{U - Q_t}{Q_t}\right) = -0.2912t + 591.03 \tag{4}$$

With these two models, the US cumulative PV installation can be projected, as shown in Figure 5. Since Q_t in the logistic growth model reflects the ratio of PV generated to the total electricity, we need data of the latter variable for future years to estimate the corresponding PV installation value. For that purpose, we adopt the recently published EIA Annual Energy Outlook 2012 Early Release,[13] which incorporates a projection of the total US electricity generation until 2035. For years since 2035, we assume a 0.8% annual increase, which is the average annual rate for the data from 2010 to 2035.

From Figure 5, we can see the main difference between the two models: the exponential model is simply based on the historic data and maintains the exponential pattern as time goes on, whereas the logistic model exerts a modulation by introducing a saturation level. For the logistic model, the growth pattern slows down when the market supply–demand relationship becomes a more critical influence. To obtain a more straightforward understanding of the current status of PV development, we present the same information in the form of the PV share of the total US electricity supply, as shown in Figure 6.

From Figure 6, we can see that if 25% of the total electricity supply is the saturation level for PV,

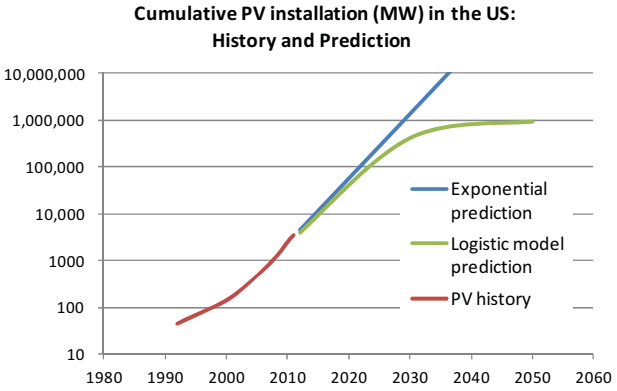

FIGURE 5 | US PV installation capacity: history and predictions based on two models.

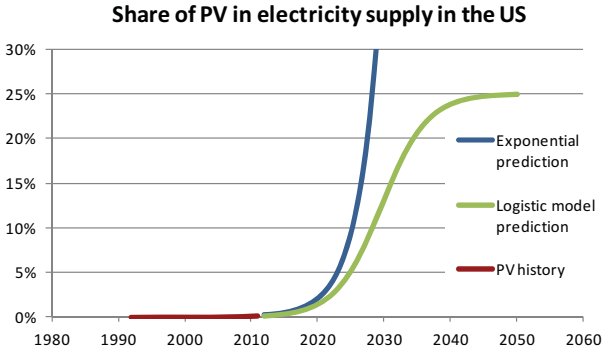

FIGURE 6 | US PV electricity share in the total national electricity supply: history and predictions based on two models.

the current achievement still resides in the 'innovators' phase.[14] Therefore, it is too early to predict an accurate date of realizing PV as a major electricity source. However, this projection provides a picture that shows how close the goal can be if we keep approaching it with the same amount of effort. On the basis of the logistic model, 24.9% of the total US electricity generation can be supplied by PV in 2049. If the exponential tendency can be maintained in the following decade, during which the two prediction models show a good match, approximately 2% share of electricity can be provided by PV, and this technology can come to next stage of 'early adopter'.[14]

To maintain the PV market growth, cost is the first issue to be considered. During the previous years of industry's development, the government played a major role by compensating for the difference between the electricity cost of PV and that of conventional sources in the form of subsidy. An electricity cost of 10 ¢/kWh is considered an average value for the current electricity sales,[13] and this is converted to a PV system cost of approximately

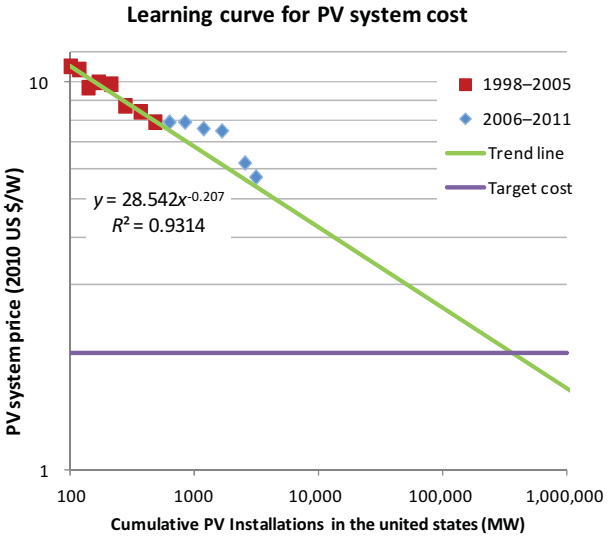

FIGURE 7 | PV system price learning curve for the United States. The learning curve (indicated as trend lin98e) is derived based on data from 1998 to 2005 because the cost over the 2006–2011 period has been influenced significantly by the temporary shortage of silicon for PV fabrication.

$2/W.[15] The conversion will be discussed later in this article.

The average PV system cost has been investigated by the Lawrence Berkeley National Laboratory, and a recent report covers data from 1998 to the first half of 2011.[16] With the cost data and the contemporary cumulative PV installation, we adopt an exponential model[17] to depict the historic PV cost and the development tendency, as shown in Figure 7. The exponential model is described by Eq. (5):

$$C_t = C_0 \times U_t^{\beta} \tag{5}$$

where C_t and C_0 stand for PV system cost at time t and a reference cost, respectively; U_t stands for cumulative PV installation at time t; and β is a parameter that characterizes the price decrease rate as market scales up.

When material supply began to catch up with market demand, PV system cost gradually became consistent with the trend line. Reflecting this point, Eq. (5) can be rewritten as:

$$C_t = 28.542 \times U_t^{-0.207} \tag{6}$$

Before the realization of grid parity, we assume that the difference between the target PV system cost of $2/W and the temporary market cost is paid by the government. Thus, the total amount of government input before grid parity can be calculated

with Eq. (7):

$$C_{tot} = \int_{U_0}^{U_g} (28.542 \times U_t^{-0.207} - C_g) dU_t \qquad (7)$$

where C_{tot} stands for the total investment from the government; U_0, U_g, and U_t stand for cumulative PV installation at a reference time, the installation goal that corresponds to grid parity, and installation as a variable, respectively; C_g stands for the PV system cost goal corresponding to grid parity.

Applying the target PV system cost (C_t) of \$2.0/W into Eq. (6), the corresponding target cumulative PV installation is calculated to be 369.1 GW, and this is the value of the variable U_g in Eq. (7). Since the most recent cost data corresponds to the first half of 2011, we consider the cumulative installation at that time as the starting value (U_0) of the integration in Eq. (7), which is 3.1 GW. Applying these values into Eq. (7), C_{tot} is calculated to be 178.3 billion dollars.

If the future PV system cost is consistent with the learning curve as shown in Figure 7 and the electricity cost of conventional sources is maintained, the required total subsidy from the government is not dependent on the PV installation diffusion pattern.[b] However, the PV installation diffusion pattern does affect the annually required subsidy. With the logistic model for cumulative PV installation and the learning curve for the PV system cost, the annual subsidy since 2012 is calculated and displayed in Figure 8. The calculation shows that grid parity can be realized in 2030, based on this set of assumptions.

The calculated annual budget for PV subsidies is in the range of two to 16 billion dollars. This high cost demands a significant portion of the total energy budget of the United States.[c] To lower the annual subsidy amount while striving for PV to account for 25% of the total US energy, PV system cost needs to decline more rapidly than the historical trend.

Although the previous PV system cost decline can be attributed to market scaling to a great extent, R&D also played a major role in historical cost decline. In the following sections, we focus on the contribution of high efficiency to low PV energy cost and future R&D opportunities to raise PV efficiency.

THE CONTRIBUTION OF HIGH EFFICIENCY TO LOW PV ENERGY COST

In general, R&D activities can lower PV energy cost in two ways: (1) by improving device or system performance and (2) by reducing manufacturing or assembly costs. Following the first approach, research that prompts innovative concepts to improve solar cell and module efficiency has led to impressive progress during the past decades (see Figure 9).[19] An example of the second approach is the improvement of growth rate of epitaxy layer to lower solar cell fabrication cost.[20]

Both approaches are necessary to lower PV energy costs, but the second approach is often seen as involving less risk and therefore may attract significant (although not necessarily sufficient) industry support. R&D activities of the first type can be more risky in terms of near-term impact. However, abandoning the first type of R&D activities will adversely affect the entire PV field development process because it will exhaust the improvement opportunities. As a result, R&D activities focusing on innovative concepts and involving higher risk are more often funded by governments.

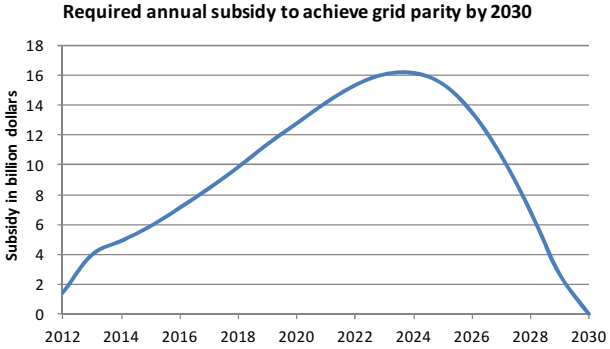

FIGURE 8 | Estimated annual subsidy for the United States based on the logistic growth model of PV installation diffusion (see Figure 5) and the system price learning curve (see Figure 7).

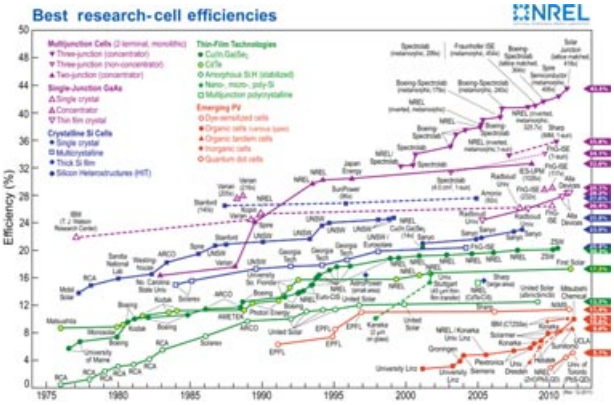

FIGURE 9 | Progress of solar cell efficiency records for different PV technologies.[19] Compiled by L.L. Kazmerski, National Renewable Energy Laboratory, Golden, CO.

Another important reason why R&D activities aiming at high efficiency should be encouraged is its impact on PV energy cost. For the quantitative analysis of this impact, we adopt the levelized cost of energy (LCOE) as the metric. LCOE incorporates operating condition variables that affect the long-term energy production and considers financial parameters that affect the cash flow during the total life cycle of the system.[d,21] In the following analysis, the value of LCOE is calculated with the Solar Advisor Model (SAM, Version 2010.4.12),[e] a performance and economic model designed to facilitate decision making in the renewable energy industry.[22]

Although the comprehensive energy conversion efficiency of PV systems can be affected by many factors, here we set module efficiency as the variable for illustration. To quantify its influence on LCOE, a reference system is specified that adopts 14% module efficiency and is installed at Phoenix, AZ, USA. The system cost includes a $1.9/W module cost and a $1.6/W cost of balance of system (BOS), and these values are mentioned as 'current best-practice costs for PV systems' for ground-mounted systems in a PV cost analysis prepared by the Rocky Mountain Institute, Snowmass, Colorado, USA.[23] The LCOE is calculated to be 10.7 ¢/kWh.[f] This LCOE of 10.7 ¢/kWh is the energy cost to the manufacturer or the investor. Compared with the electricity sales price, this LCOE does not incorporate tax considerations. For instance, an estimate of the market price can be 17.9 ¢/kWh, derived based on 10.71¢/kWh for the manufacturer, 8% state tax, and 35% federal tax. Considering a comprehensive tax rate of 40% that combines state and federal taxes, and assuming a good linearity between LCOE and total system cost in units of $/W,[24] an average market electricity price of 10 ¢/kWh is converted to a $2.0/W system cost. This is consistent with the target PV system cost we set in the previous section.

For an area-constrained installation, some costs are fixed. These include expenses on structuring installations, such as racking, site preparation, attachments, etc., and business processes, such as financing and contractual costs, permitting, interconnection, etc. For the reference system, these expenses share approximately one-third of the total system cost, as shown in Figure 10.[23,24]

While maintaining the values of other parameters, raising module efficiency can spread these fixed expenses over larger volumes of energy and therefore lead to a lower LCOE. The calculation result is displayed in Figure 11.[g,h]

In Figure 11, each curve represents a constant module cost in units of $/W, which means that the

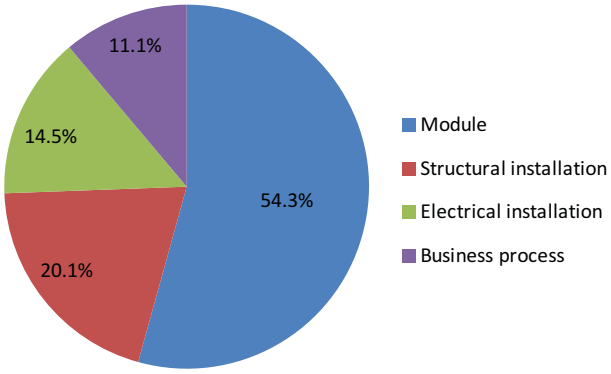

FIGURE 10 | System cost breakdown of a representative commercial PV installation in 2010.[23]

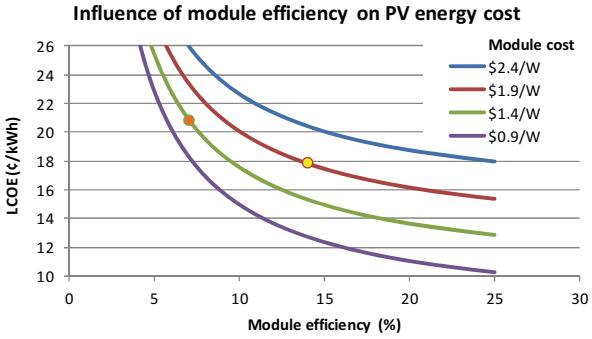

FIGURE 11 | LCOE as a function of module efficiency and module price. All systems are flat plate PV installations with fixed tilt at Phoenix, AZ, USA. (Reprinted with permission from Ref 24. Copyright 2011, Elsevier.)

module price in units of $/m^2 is linearly proportional to module efficiency. By comparing across different curves, we find that the linear relationship between unit area module cost and module efficiency is not a necessary condition for high efficiency modules to win over low efficiency ones. For instance, if we start from 7% efficiency and $1.4/W module cost (indicated by the orange spot in Figure 11) and increase efficiency to 14% and the associated cost to $1.9/W (indicated by the yellow spot in Figure 11), which means that efficiency doubles and unit area cost is increased by a factor of 2.7, the LCOE still decreases from 20.9 to 17.9 ¢/kWh (a 15% decrease).

The analysis shows that higher module efficiency leads to a lower PV LCOE, and the reason resides in the area-related and fixed BOS expenses. Therefore, the greater the ratio of these expenses to total system cost, the more sensitive the LCOE is to module efficiency. In tracking PV systems (flat plate PV or concentration PV), the extra cost related to trackers increases this ratio, and accordingly the LCOE is more dependent on module efficiency. More

details about the desired module efficiency for different system configurations are to be discussed in the last section.

R&D OPPORTUNITIES FOR HIGH EFFICIENCY PV

PV efficiency can refer to many components of a system, all of which affect energy conversion. Although the most straightforward metric is system energy conversion efficiency over the life cycle of the system, the sunlight-to-electricity (AC) process needs be broken down to several parts where specific R&D activities can be focused. Accordingly, R&D opportunities can be found at different levels: solar cell efficiency, PV module efficiency, and long-term operational reliability, for example. Below, we discuss R&D opportunities at diverse levels for high efficiency PV technologies based on Si, thin film II–VI, GaAs, and multi-junction III–V materials.

As the dominant solar cell material in PV industry, crystalline Si has achieved 25% and 22.9% cell and module efficiencies, respectively.[i,25–27] The record cell efficiency is at 84% of its theoretical efficiency limit of 29.8%,[28] and the record module efficiency is 92% of the record solar cell efficiency. These great efficiencies require very high material quality that provides long initial carrier lifetimes, a well-controlled pure growth environment that maintains the long lifetimes during cell fabrication, and delicate cell structures. All of these factors can greatly increase cost and are not compatible with high volume manufacturing, given fabrication technologies that have already been developed for use by the microelectronics industry.

As a relatively new field, the PV industry evolved mostly by adopting the available techniques and equipment of microelectronics. Thus, goals to increase efficiency largely avoid designs, which would depend upon radical alternations of microelectronics manufacturing methods and/or equipment. Despite the achievement of high efficiencies at both the cell and the module levels during the 1990s, the current PV market is dominated by Si-based modules[j] with efficiencies in the range of 13–17%. With the current practical constraint on efficiency, the PV industry has still experienced impressive growth in the volume of production, with 38% yearly market expansions on average during the past two decades.[29] Having opened the door of the market, attention is now focused on increasing performance to lower the cost of PV energy supply and thereby widen its market.

Si materials for PV fabrication can be generally divided into two categories: crystalline and amorphous. According to the grain size of the crystal, further sub-categories are as follows: single-crystalline (>10 cm), multi-crystalline (1–100 mm), poly-crystalline (1–1000 μm), and nano-crystalline (<1 μm). From an engineering point of view, each type has potential to achieve higher efficiency at both the cell and module level. The limit of achievable efficiency, however, is intrinsically set by material quality. Here, we focused on sc- and mc-Si cells and modules of high material quality.

The current record efficiencies for mc-Si cells and modules are 20.4% and 18.2%, respectively.[27,30] Compared with sc-Si record results, mc-Si devices are 4.6% and 4.7% (absolute) lower in efficiency at the cell and module levels. Efficiencies of most commercial sc- and mc-Si modules, however, differ to a small extent (typically the difference is 1–1.5%) because fabrication procedures are largely the same for both materials, during which the long lifetimes initially observed for the high-quality sc-Si material fall off (due to accumulated defects along the way).

The dominant Si materials in commercial applications are sc-Si of Czochralski (Cz) type and mc-Si grown by the block-cast method. Compared with float zone (FZ) sc-Si, Cz-Si is widely used in the industry due to its availability. However, Cz-Si contains a high concentration of oxygen, which is not active by itself but can lower the lifetimes after forming oxygen complexes in the material.[31] Compared with sc-Si, mc-Si has crystal defects such as grain boundaries and dislocations; moreover, high concentration metals that are introduced in faster solidification will aggravate recombination and lower the lifetimes.[32] In large volume production, the growth environment has more contamination sources, and the impurities and defects are more active after high temperature processing. These factors result in a two-order reduction for the commercial substrate lifetimes, compared with high-quality FZ-Si. For this reason, future efforts at the material level will focus on growth environment control. Besides the condition control during growth, material quality improvement opportunity is also present afterward. A currently existing example is hydrogen passivation, which has played a significant role in boosting commercial mc-Si cell efficiency.[33]

Although most commercial companies manufacture c-Si modules of efficiency in the range of 13–16%, one exception is SunPower, whose commercial products (e.g., E20/327) realize 22.5% efficient solar cells and have achieved module efficiency of more than 20%.[34] The high module efficiency is mainly

attributed to long lifetimes of the carriers and back contact cell design,[35] which avoids the 7% shading loss for cells with screen-printed contacts.[32] This achievement indicates another more radical R&D approach: instead of applying modifications while maintaining the main frame of the manufacturing line, newly designed lines can be developed for new concepts.

Rather than improving the growth conditions and modifying the structure for the traditional thick Si cells, another more radical R&D approach is thin film Si cells. The most apparent advantage of thin film cells is the cost saving on material; moreover, high cell efficiency is another great attraction. The principle of the high efficiency resides in less bulk recombination due to a reduced distance; the minority carriers need to travel before they arrive at the depletion region. The realization of this concept, however, enhances the necessity of two other improvements: surface passivation and light trapping. As the thickness is reduced, the density of minority carriers generated close to the surface increases; therefore, cell efficiency is more dependent on the surface passivation. Si oxide and Si nitride have been used for that purpose.[32] A collection of improvement innovations can be found in literature.[36]

Another improvement related to thin film Si cells concerns light capturing. Si has an indirect band gap and the resultant low absorption coefficients require a longer path for sunlight to be highly utilized. As the physical thickness of a Si cell decreases, cell structure needs to be adjusted to increase the effective path length, and this is the basic concept of light trapping. One option of light trapping is to utilize interference in a Si oxide–metal structure on the bottom.[37] Another option is texturing the front surface. Pyramids on the surface can alter the propagation direction of the sun's rays in the solar cell and therefore lengthen the optical path. When texturing on the front side is available, the rear side reflector can be adjusted such that total internal reflection (TIR) can occur for multiple passes. Another function of texturing is that the reflected rays at one pyramid strike a neighboring pyramid, allowing additional light to be captured.

Although the high efficiency feature of thin film Si cells necessitates improvements on surface passivation and light trapping, the realization of its low cost requires innovations in wafer or epitaxy layer processing. To achieve thin Si cells, a straightforward approach is to reduce the thickness of the wafer. Currently, the thickness of commercial crystalline Si wafers is in the range of 180–210 μm[32]; future improvements are likely to lead to wafer thickness below 100 μm.[38,39] This change enhances the requirement of wafers' mechanical strength, and caution must be exercised in subsequent processing steps. For instance, sawing technologies need to be improved, as well as new screen printing techniques (or alternatives to fabricate the contacts) and better handling and shipping.

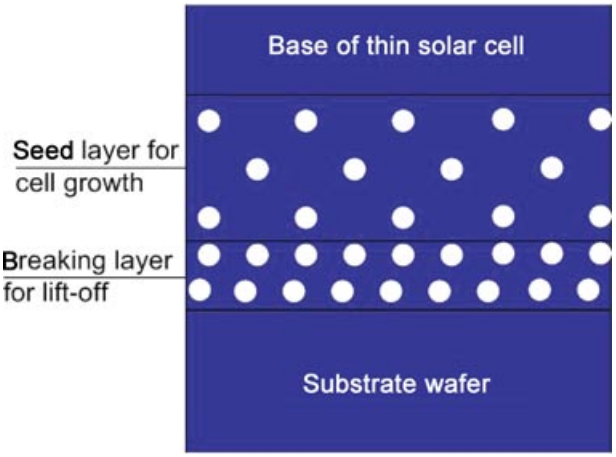

FIGURE 12 | Schematics of thin film Si growth structure using 'layer transfer' technology. The breaking layer has a thickness of 350 nm and a porosity of 55%; the seed layer has a thickness of 1200 nm and a porosity of 20%.[41] The drawing is for illustration purpose but not to scale.

The thin wafer approach is based on the assumption that the wafer is one functioning component of the solar cell. Overthrowing that assumption, there is a second approach that adopts the concept of 'layer transfer'.[40,41] This approach allows the thin solar cells to be lifted off the substrate wafer, which can be used multiple times. A mesoporous double layer between the substrate wafer and the thin solar cell is the innovative component that allows the layer transfer, as shown in Figure 12. Currently, a record efficiency of 19.1% has been achieved on thin Si solar cells fabricated with this technology.[41] This achievement is a demonstration of realizing high efficiency in thin Si cells, and further improvement on performance is expected. However, the current laboratory fabrication steps are complex, and continuous R&D activities are required to simplify manufacturing steps for high volume production.

Different from c-Si cells described above, which involve making ingots and slicing them into wafers, some other solar cell materials can be deposited directly on substrates or superstrates as films. These materials have direct band gaps, or greater absorption coefficients, which means that they can be very thin—on the order of 1 μm compared with 100 μm for c-Si—to absorb most of the sunlight. Therefore,

solar cells made from these materials are named thin film devices. Two thin film devices that have been extensively explored and have achieved significant progress are copper–indium–gallium–(di)selenide (or more simply, CIGS) and CdTe.

With properties that are advantageous for PV applications, CIGS cells have been researched since the early 1970s. This research has led to improved material deposition methods, better device structure designs, and more cost-effective manufacturing procedures.[42] Here, we only mention the problems to be solved for the next-generation high efficiency CIGS thin film cells.

The current record efficiencies for CIGS are 19.6% and 15.7% at the solar cell and module levels, respectively.[27,43] These achievements, however, have been partially based on empirical improvements, and the underlying principles are not yet fully understood. Reproducibility of large volume manufacturing with current achieved performance and further efficiency improvement will depend upon a more solid understanding of the working mechanisms. For instance, it is empirically known that the presence of Na in CIGS is beneficial for PV performance.[44] However, the principle underlying the effect of Na has not been fully understood, although a tentative explanation that Na helps passivation on grain surface is being investigated.[45–48] Another puzzle concerns the influence of grain size on CIGS cell performance. Different from c-Si solar cells, whose performance is directly related to grain size (due to the correlated recombination), CIGS solar cells display insensitivity to grain size.[42] Although tentative explanations are given, the underlying principles are not yet known.[50–55] As with other solar cells, reducing recombination by improving material quality should be a fundamental R&D direction for CIGS solar cells. For that purpose, modeling of the grain boundary behaviors based on a detailed understanding of the phenomenon is necessary.

Another R&D focus is to develop a better substrate. Because CIGS film growth occurs on top of a substrate made of a different material, the thermal expansion coefficients of the substrate and the CIGS film should be the same in order to avoid stress. A good match of this parameter has been found with soda-lime glass.[42] However, this glass begins to soften at 500°C, whereas ideal solar cell fabrication needs an operating temperature above that point.[42] This conflict does not greatly affect the record cell performance because the cell has a small area and its performance is not very sensitive to glass deformation. However, a glass with higher temperature resistance will be necessary for high efficiency large volume production.

Compared with c-Si solar cells, CIGS involve multiple types of materials in the fabrication. This diversity necessitates more sophisticated control of material deposition parameters and diagnostic tools to identify problems. Developing a comprehensive design of deposition equipment, manufacturing and diagnostic tools could greatly improve large volume production, in which reproducibility and uniformity are desired.

A second type of extensively investigated thin film solar cells is based on CdTe. The record efficiencies of CdTe are 16.7% and 12.8% at solar cell and module levels, respectively, both of which are 2.9% (absolute), lower than that for CIGS.[27] Notwithstanding its lower efficiency, CdTe experienced greater market penetration and developed more mature manufacturing techniques. The biggest CdTe commercial company, First Solar, has achieved a total manufacturing capacity of 2.4 GW.[55] This company claimed that its FS-390 series has a module efficiency of 12.5%, very close to laboratory record.[56]

The current CdTe solar cell structure and fabrication conditions are based on empirical learning to a great extent, together with a basic understanding of this material. Although the band gap property of CdTe allows its theoretical solar cell efficiency to be above 30%, cell efficiency in the laboratory has hovered at 16.7% for a decade. The barrier has been commonly attributed to low open-circuit voltage (V_{oc}) and fill factor (FF). To raise this cell efficiency, a promising approach is to improve the quality of the CdS/CdTe junction to achieve lower forward-current recombination. An equally promising direction is to focus on reducing recombination states at the grain boundaries as well as in bulk.[57] Besides recombination problems, another challenge is to overcome self-compensation in p-type CdTe doping to achieve the desired doping concentration.[58,59] Each of these problems requires basic research in order to realize a deeper understanding of the material's properties.

Another significant focus for CdTe solar cells is to stabilize long-term performance. A widely observed reliability issue for CdTe solar cells concerns the barrier at the back contact. Although tentative explanations attribute the problem to copper used in the back contact, a better understanding is needed.[60]

Besides Si and II–V materials, single-junction solar cells have also been researched for and demonstrated by III–V materials, and GaAs stands out with high cell efficiency that can be attributed to its direct band gap with a value suitable for PV application. However, GaAs solar cells have not been considered for wide terrestrial application because the material is very expensive. This restriction has been recently

alleviated by the noticeable progress of adopting 'lift-off' technology in GaAs cells.[61] This lift-off technology allows the expensive substrate to be re-used after the epitaxial film is removed, and therefore the material cost is greatly reduced. Although not many fabrication details have been released by Alta Device, the commercial company that has deployed R&D on this topic, the basic concept is considered similar to the 'layer transfer' for Si thin cells. With this technology, a cell efficiency of 28.3% has been achieved; this is not only a new record for GaAs cells but also a record for all types of single-junction cells.[27] Furthermore, the efficiency of the modules made of thin film GaAs cells by the same company has created a record of 23.5%, which for the first time surpassed the 22.9% single-junction solar module efficiency that had been maintained by Si modules.[27] The new high cell and module efficiencies open another promising avenue for low cost high efficiency PV in terrestrial applications. Research priorities include: (1) maintaining the high efficiency of solar cells grown from the same substrate; (2) exploring the limit of substrate re-use; (3) raising the growth rate of metal organic chemical vapor deposition (MOCVD) currently being used for epitaxial layer growth, or exploring other high-speed growth techniques; (4) producing larger modules of good uniformity; and (5) developing manufacturing equipment and procedures for high volume production.

Although single-junction solar cells of different materials are being improved for higher efficiency, multi-junction solar cells have also demonstrated a great progress. III–V materials are extensively explored for this purpose because they provide wide options of band gap and lattice constant for system optimization. Because of the high cost related to expensive materials and complex fabrication steps, multi-junction solar cells are usually adopted in concentrating PV (CPV) configurations for terrestrial application.

Efforts to incorporate concentrators into PV modules date back to the 1970s.[62] The basic idea is to use low-cost optical concentrators to reduce the required area of solar cells, which are more expensive than optics. Using the ratio of a concentrator's active area to a solar cell's area as the standard, CPV can be categorized as low-X (1–10X), mid-X (10–100X), and high-X (100–1000X).[k] In this section, we review the current status and potential R&D opportunities for the currently dominant type, high-X CPV.

The most commonly adopted III–V multi-junction solar cells have three sub-cells, and their cost is two orders higher than that of Si cells. High-X concentrators may therefore be necessary for these multi-junction solar cells to compete with Si cells. Moreover, high-X CPV depends upon high-accuracy tracking, which introduces a significant additional cost. To compensate for the high costs of both solar cells and trackers, the commercial CPV systems in the market are usually around 500X.

Triple-junction concentration solar cells have achieved a record efficiency of 43.5% at 418X.[27] Applying the principle of detailed balance, an ideal triple solar cell with band gaps of 0.94, 1.34, and 1.86eV[63] that are optimized for current-match conditions can operate with an efficiency of 55.9% at the same concentration. The realized solar cell efficiency corresponds to 78% of the theoretical limit. Researchers continue to investigate even higher cell efficiency by applying alternative growth techniques to relax the restriction posed by lattice match so that the band gaps can further approach the theoretical optimal values. One example is the inverted lattice-mismatched GaInP/GaInAs/GaInAs solar cell that can tolerate more lattice mismatch by growing the epitaxial layers inversely and gradually increasing the order of lattice mismatch.[64,65] This growth technique can realize band gaps closer to the theoretically optimal values and therefore higher solar cell efficiency. Efficiency (40.8%) at 326X has been achieved,[64] and 45% efficiency is expected with continued development.[66] Although noticeable progress has been observed on triple-junction concentration solar cells under standard measurement conditions, their performance in long-term operation needs more careful assessment.

Triple-junction solar cells adopted in commercial CPV systems utilize a monolithic structure with the three sub-cells connected in series. Both the design and measurement of these solar cells are based on a reference spectrum, usually ASTM G-173-03 Direct.[67] However, the real spectrum can experience dynamic variation. The current match among the three sub-cells, or at least between the top and middle sub-cells, can be achieved under the reference spectrum, but it cannot be maintained constantly in real operation. Figure 13 shows the calculated efficiencies under different spectrum conditions for a triple-junction monolithic solar cell with band gaps optimized for current match.

The solar cell efficiencies in Figure 13 are calculated for 100X concentration and are based on the detailed balance model.[63,68–70] The purpose of Figure 13 is not to show the absolute value of the efficiency but to demonstrate the large efficiency deviation for a triple-junction monolithic solar cell; this great deviation is due to current mismatch caused by spectrum variation. In Figure 13, the red curve is derived based

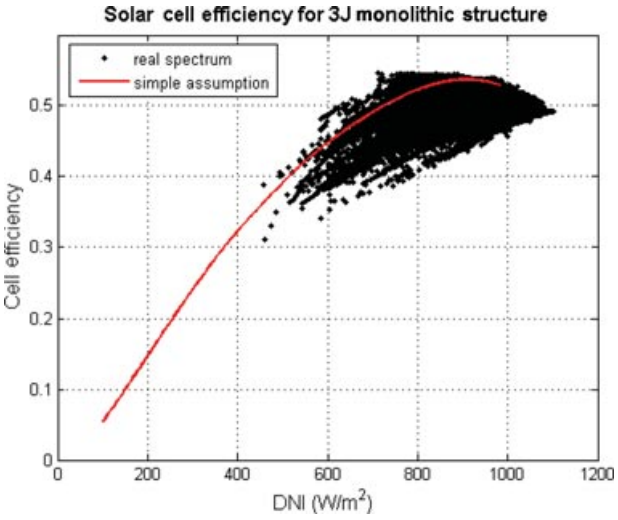

FIGURE 13 | Calculated efficiencies for ideal two-terminal triple-junction cells at 100X. The black dots are calculated using real spectrum at Golden, CO, USA in 2002. The red line is calculated under a simple assumption that air mass is the only factor that affects spectrum.

on the assumption that the spectrum is only affected by the air mass, and all other parameters that influence the spectrum are constants. The black dots are derived with the available real spectra measured in 2002 for Golden CO, every 60 seconds. The variation range can be greater than 20% even at high irradiation ranges. In Figure 13, efficiencies are not plotted in the low irradiation range because spectrum data are not available under those conditions.[71,72]

As CPV plays a more serious role in the PV market, the spectrum sensitivity issue has garnered more and more attention. Exploring research pertinent to this topic can be found in recent publications by academic institutes and commercial companies.[73–78] Considering the significant influence of spectrum variation on solar cell efficiency and the limited spectrum data resources, it would be valuable to deploy more R&D activities to quantify spectrum sensitivity. The research can indicate the proper locations for CPV installations, where dynamic spectrum variation is observed to be comparatively low. For those locations with relatively stable spectrum conditions, the band gaps of the three sub-cells may be tuned for optimal energy generation in long-term operation.

Another focus of CPV research is to further split the spectrum, using four, five, or even six junctions to absorb the broadband spectrum.[79] Combining this strategy with efforts to adjust band gaps to approach the optimal values can lead to future solar cell efficiency increases. However, actual operating conditions suggest that expanded spectrum splitting may create more problems than it solves. Highly dynamic spectrum variation raises doubt about the value of developing four-, five-, or six-junction solar cells, at least in a monolithic structure for terrestrial application. Figure 13 shows analyses only for triple-junction solar systems because they are the actual structures being adopted in the existing CPV market. It is predictable that, as the divisions of the spectrum increase, the solar cell efficiency will have a higher sensitivity to spectrum variation and therefore will experience more energy loss when the spectrum deviates from the standard. It remains to be seen if the efficiency gain by increasing the number of sub-cells predicted under the standard spectrum can be realized in field applications when dynamic spectrum variation occurs. For example, a switch from three to four sub-cells results in a theoretical efficiency gain of 8% (relative) under the standard spectrum.[63,68,80] However, in the field, a higher sensitivity to spectrum variation may make the energy production of the four-cell system close to or even lower than that of the three-cell system.

Different from monolithic solar cells which split the spectrum in a vertical or a series way, another concept called 'lateral spectrum splitting' has recently been applied in some R&D projects.[81,82] The basic principle is to split the spectrum using additional optics before the sunlight arrives at solar cells designed for different wavelength ranges. With the lateral spectrum splitting approach, the cells can be fabricated and optimized separately, and this can completely or partially release the restrictions of current match or lattice match. 36.7% and 38.5% record submodule efficiencies have been demonstrated on prototypes of different structures.[83,84] However, to prove the feasibility of this concept, more R&D efforts are required on the variation design of the electronic circuit because multiple outputs are present in the lateral structure compared with one output in the monolithic structure; also R&D efforts are required on module structure optimization because more components are present in the lateral structure than in the monolithic structure.

Besides spectrum variation, another important issue that affects the performance of concentration triple-junction cells is the nonuniformity of illumination. In both the design and measurement phases of such a solar cell, it is assumed that the illumination is uniform across its surface. Although this condition is satisfied for flat plate PV, it cannot be guaranteed when a cell is assembled together with a concentrator and installed in the field. Although secondary optical components in high-X CPV are designed to homogenize the rays that pass through the primary

concentrators, the designs are based on perfect tracking. When a tracking error occurs in field operations, the uniformity found in ideal tracking is not necessarily maintained. The nonuniformity of illumination directly causes voltage difference across a solar cell, which leads to lateral current flow and can be reflected as low FF on the I–V curve. This effect was analyzed as early as 1960 on a single p–n junction[85] and discussed in the 1990s on a monolithic two-junction solar cell.[86] The influence of nonuniform illumination on monolithic multi-junction solar cells necessitates three-dimensional analysis because the junctions are affecting each other when connected in series. Recent research suggests that in a CPV module utilizing secondary optics, the FF decreases by more than 4%, whereas the short circuit current or Isc decreases by less than 2% at a tracking error of 0.5°.[87] Considering the potential gain by improving the FF in real operating conditions, more R&D activities can be deployed to design secondary optics incorporating different tracking errors.

The above-mentioned issues concern CPV solar cell efficiency, but a large portion of energy is also lost on optics before it can even reach the cell. According to their working mechanisms, CPV concentrators can be categorized to two main types: reflective and refractive, as shown in Figure 14.

Compared with a refractive concentrator system (Figure 14b), a reflective concentrator system (Figure 14a) has the main advantage of compactness; the thickness of the module can be much smaller than the concentrator opening. This can potentially save material cost and facilitate fabrication, shipping, and installation. However, a reflective concentrator system has two more optical components where extra losses occur. One is the top glass cover, where an 8% optical loss occurs. The other is the secondary mirror, where another 8% optical loss occurs.[88] Considering the higher optical efficiency, the following discussion is based on refractive concentrator systems.

Refractive concentrators follow Snell's Law. A traditional smooth convex lens has a thickness proportional to the diameter of the lens. For lenses with diameters in the order of 10 cm, smooth lenses are too heavy and costly. To solve that problem, CPV modules usually adopt Fresnel lenses that have functioning grooves and dispose the chunk volume.

The front side of a Fresnel lens is usually designed as a flat surface for cleaning convenience and to avoid dust accumulation. The Fresnel loss at the air–lens interface is 4%. At the rear surface of the lens, only rays passing through the optics axis have zero incidence angles at the lens–air interface; other rays are tilted and therefore have greater Fresnel losses. For a

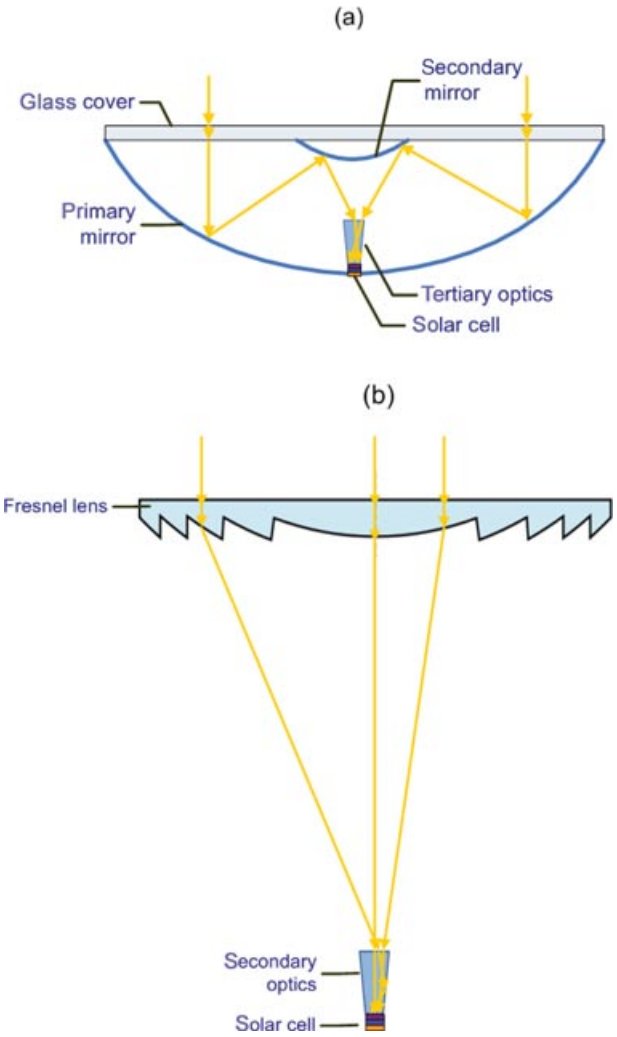

FIGURE 14 | (a) A typical reflective CPV module structure; (b) a typical refractive CPV module structure.

Fresnel lens with the *f*-number equal to 1, the loss is 5%. Compared with a smooth lens, extra losses on Fresnel lenses occur because of flaws at the non-ideal grooves, including non-zero draft angles and round corners.[89] Sunlight striking flawed surfaces is scattered and cannot be guided to the target solar cell. For instance, a round corner of 5 μm radius and 3° draft angle can cause a 5% scattering loss.

Considering the losses mentioned above, 87% of the direct normal irradiation (DNI) can pass through a Fresnel lens. However, these rays cannot be fully guided to the target solar cell because of the divergence angle of DNI, tracking errors, and chromatic aberration.[1] The significant amount necessitates secondary optics. For an ideal solid secondary optics, the rays can either go through it without hitting the wall or strike the wall with an angle that satisfies

TIR. Only considering the 4% Fresnel loss at the top surface and assuming zero absorption in the solid, the comprehensive optical efficiency is 83% at perfect system pointing.

Although CPV trackers are still under development for more stable performance under diverse conditions, it is difficult to accurately quantify the frequency of tracking errors in field operation at this moment. For an optimistic estimation, we assume 5% efficiency loss due to pointing error, which can cause decline of both FF and Isc of the solar cells.

The sophisticated module structure and the accompanying high risk make high-X CPV more complex than choosing its higher cell efficiency. Starting from 40% solar cell efficiency, we can estimate the comprehensive efficiency based on the above discussion. The estimated values for the influencing factors include: (1) a 10% loss due to current mismatch among sub-cells under dynamic spectrum variation; (2) a 17% optical losses at ideal system pointing; and (3) an extra 5% loss when considering the pointing errors in long-term operation. These values lead to a 28.4% efficient CPV module. However, this efficiency is based on several assumptions, including ideal secondary optics, well-controlled system pointing, and spectrum sensitivity derived based on limited spectrum data. Even this seemingly high module efficiency does not guarantee CPV's superiority over flat plate systems because CPV can only utilize the direct beam and the diffuse light is wasted. Only considering the usable irradiation and the module efficiency, a CPV system using 28.4% efficiency modules generates the same energy as a tracking flat plate system using 21.9% efficiency modules of the same active area, for a location where DNI is 77% of the global normal irradiation (GNI). Seventy-seven percent is a representative value for the annual DNI–GNI ratio at lots of locations in United States, including Phoenix, Arizona, and Las Vegas.[m]

For future CPV modules of higher efficiency, there can be two major R&D directions: small units and low-mid X concentrations. The small unit concept means that each submodule has a small active area, creating several advantages. The first is at the optics level. The thickness of a smooth convex lens is proportional to its diameter, so a small dimension of the submodules of a CPV system allows smooth lenses to be adopted; therefore, the scattering loss at the non-ideal grooves of Fresnel lenses can be eliminated. The second advantage is at the electrical level. As the submodule area decreases, the resistive loss decreases. This is because the output power from a submodule is proportional to its operating current, or its active area, whereas its resistive loss is proportional to the square of its operating current. The third advantage is at the thermal level. For the same concentration, small submodules correspond to small solar cells and a smaller dimension of the cells is beneficial to heat dissipation. This is good because a cell's efficiency is inversely proportional to its operating temperature. The fourth advantage is at the material level. For the same concentration, small submodules correspond to thinner modules. Therefore, materials can be saved and lower cost is required for shipping and installation. A commercial company named Semprius has adopted this small-unit concept and applied smooth lenses in the CPV modules. A recent measurement demonstrated 33.9% efficiency of the Semprius modules under the standard testing conditions.[90]

Accompanying the advantages, there are two new problems. First, for the same active module area, small units mean a greater amount of the units, which may increase costs related to assembly. Currently, this problem has been solved by a technology called 'micro-printing', which is adopted by Semprius.[91,92] This technology can process many tiny solar cells at the same time. The other problem is the increased sensitivity to alignment error. Misalignment in actual manufacturing or assembling can cause higher losses for small submodules because a certain absolute value of the misalignment corresponds to a greater fraction of the operation dimension. It is yet to be proven that the high alignment accuracy can be maintained in both laboratory conditions and real operation.

Another R&D direction to achieve higher CPV module efficiency can be switching from high to low-mid concentration. Lower concentration can eliminate the use of secondary optics and/or reduce the sensitivity to system pointing. The success of this variation is intrinsically dependent on the cost decline of the multi-junction solar cells.

Current technology used to fabricate III–V solar cells is MOCVD and most of the equipment is made by a commercial company named Veeco. Veeco is developing new growth tools to realize fast growth of crystalline layers and reduce the fabrication cost of the solar cells.[93] Another exploration direction is to adopt an innovation concept of 'lift-off' that allows multiple uses of expensive substrates for growth of thin epitaxial layers. Research on this topic has been mentioned in previous paragraphs for thin Si cells[40,41] and thin GaAs cells.[61] For multi-junction cells, the micro-printing technology of the same concept has been adopted by Semprius and it allows the transfer of the tiny cells away from the growth substrate, indicating the potential of substrate re-use.[94]

TABLE 1 | Absolute Values of Efficiency Achievements for Different PV Technologies

	Theoretical cell (η)	Laboratory record cell (η)	Laboratory record module (η)	Market module (η)
sc-Si	29.8%[1]	25.0%	22.9%	14–17%; 20%[2]
mc-Si		20.4%	18.2%	12–15%
CIGS	31.6%	19.6%	15.7%	11–13%
CdTe	30.3%	16.7%	12.8%	11–12%
GaAs	31.2%	28.3%	23.5%	NA[3]
Multi-J	55.9%[4]	43.5%	33.9%[5]	25–30%

1The limit for Si is based on the detailed balance model but also incorporates the absorption coefficients and carrier lifetimes.[28] The theoretical limits for other materials are calculated based on detailed balance model and the only considered material parameter is the energy band gap.
[2]The 20% module efficiency is based on back-contact solar cell structure, so this value is listed separately.
[3]Commercial products were not available at the time of this article.
[4]For comparison purpose, this value is calculated for the same concentration level as the measurement condition for the record triple-junction solar cell: 418X AM 1.5 Direct.
[5]This new record was based on tests at the Instituto de Energía Solar at the University of Madrid, Spain.[90] All the other record efficiencies are cited from the Solar Cell Efficiency Tables being updated in Progress in Photovoltaics: Research and Applications.[27]

SUMMARY AND DISCUSSION

During the past two decades, the PV industry has experienced dramatic growth, which was triggered by strong policy support and accelerated by increased economies of scale and technology improvements. Although the exponential diffusion pattern brought by the diverse efforts has pushed PV to set out on the journey to becoming a major electricity source, it is still in the innovator phase. With the historic PV installation data and a logistic model, it is predicted that PV can achieve a 25% electricity share in the United States by 2050. To realize this target, numerous subsidies are required from the government, if the future cost of PV systems starts from the currently observed average value of $5.7/W and follows the 13.4% learning rate that is demonstrated by history. In order to help the PV industry achieve sustainable progress without relying on the large subsidy from the government, more radical decline of PV system cost is needed. Although the influence of market scaling is relatively stable and predictable, we can find more exploration space from the R&D side. In this article, we focus on R&D opportunities for high efficiency PV, following a quantitative proof of the value of high module efficiency in lowering PV energy cost.

Table 1 presents the theoretical efficiency limits for solar cells of different materials and their current achievements. Table 2 presents the same information with relative values by comparing the achievement to the theoretical limit and the achievements between different levels. In the last column of Table 2, the values are derived by dividing the highest commercial module efficiencies by the laboratory module efficiency records. In the previous section, we detailed the R&D opportunities for PV technologies based on different materials. Here, we provide a general discussion by looking into Table 2.

TABLE 2 | Relative Values of Efficiency Achievements for Different PV Technologies

	Laboratory cell/limit cell	Laboratory module /laboratory cell	Commercial module/laboratory module
sc-Si	84%	92%	87%
mc-Si	68%	89%	82%
CIGS	62%	80%	83%
CdTe	55%	77%	94%
GaAs	91%	83%	NA
Multi-J	78%	78%	88%

As the most developed material, sc- Si has realized very high achievements at multiple levels, indicated by the values in Table 2. The 68% ratio for mc-Si of the laboratory cell efficiency to theoretical efficiency is relatively low, and it is intrinsically caused by the lower material quality of this type of Si. The identified R&D opportunities for future high efficiency Si include mild modifications based on current solar cell structure and exploration of thinner cells. The R&D opportunities for Si PV are summarized in Table 3.

For thin film CIGS and CdTe, both materials displayed low ratios between the laboratory cell efficiencies and the theoretical limits. One reason is the growth methods: deposition on noncrystalline growth substrates can achieve low cost but also leads to low crystalline quality of the materials. Furthermore, the main reason of the relatively low thin film cell efficiencies is limited fundamental understandings of material characteristics. More details are summarized in

TABLE 3 | Summary of R&D Opportunities for Different PV Technologies

PV technologies	R&D opportunities
Silicon	• Thick cell: Better control of growth conditions and after-growth passivation for longer carrier lifetimes; back-contact design to eliminate shading loss • Thin cell: Improve and transfer the 'lift-off' technology from laboratory to high volume production; develop thin wafers of high mechanical strength; improve processing technologies for thin wafers, including sawing, handling, shipping, screen-printing, etc.; improve surface passivation and light trapping
CIGS	• Principle understanding of materials: Explore fabrication recipe, including the influence of Na, grain size; find substrate materials with more proper thermal expansion coefficients • Laboratory-industry transfer: Develop and improve fabrication equipment, manufacturing and diagnostic tools for high volume production
CdTe	• Principle understanding of materials: Improve CdS/CdTe junction quality for lower forward-current recombination; reduce recombination at grain boundaries and bulk; solve the problem of self-compensation of p-type CdTe doping; understand and solve the cell degradation problem
GaAs	• Improve 'lift-off' technology: Achieve high repeatability of cell efficiency for samples made from the same substrate; explore the limit of substrate re-use • Laboratory-industry transfer: Develop fast growth deposition; produce large modules of high uniformity; develop manufacturing equipment and procedure for large volume production
multi-J	• Solar cell: New fabrication method to solve the lattice constant match restriction problem; explore spectrum sensitivity issue • Module structure: Develop small submodules and pertinently increase alignment accuracy and assembling efficiency; develop modules of low to middle concentration, mainly depending on the 'lift-off' manufacturing for low cost cells

Table 3. The 94% ratio between the commercial module efficiency and the laboratory record module efficiency is quite noticeable, and this achievement can be attributed to extensive R&D of module fabrication that comes along with active development of commercial products.

GaAs has demonstrated the highest ratio between the laboratory cell efficiency and the theoretical limit. The lift-off technology provides the possibility of adopting the high efficiency GaAs cells in terrestrial applications. Future R&D foci include further improvements on this technology to achieve high repeatability of performance of cells that are made on the same substrate and efforts to transfer the technology from laboratory to high volume production.

Multi-junction cells have achieved the highest efficiency among all types of solar cells. Further improvement of cell efficiency can focus on releasing the restriction posed by the monolithic cell structure, which requires lattice constant match and therefore limits the band gap optimization. Another restriction posed by the monolithic structure is current match. Pertinent to that issue, future R&D is needed to quantify the influence of spectrum variation on long-term performance of these cells. Multi-junction cells are currently applied in high-X CPV configurations. As shown in Table 2, the ratio between the laboratory modules and the lab cells are relatively low. This can be mainly attributed to the multiple optical components necessitated by the high concentration level. Compared with flat plate PV modules, CPV modules have more opportunities to boost their efficiency by improving module structure. Details are listed in Table 3.

Finally, we have a more comprehensive discussion about the future high efficiency and low cost PV technologies. Starting from the target, we set the LCOE to be 10 ¢/kWh and draw curves reflecting the relationship between module cost and module efficiency, as shown in Figure 15.[n] Different curves correspond to three system configurations: fixed flat plate,

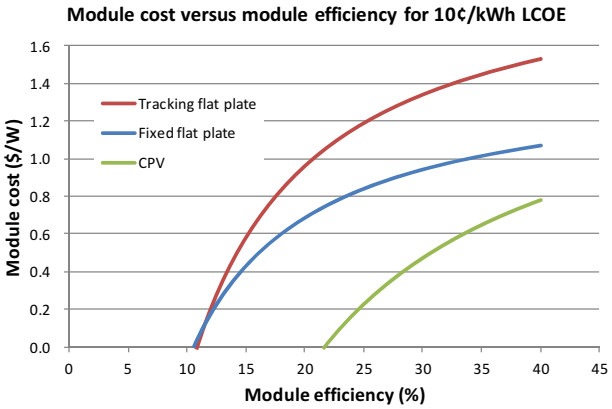

FIGURE 15 | The relationships between module cost and module efficiency at a target LCOE of 10 ¢/kWh, for fixed flat plate, tracking flat plate, and CPV systems.

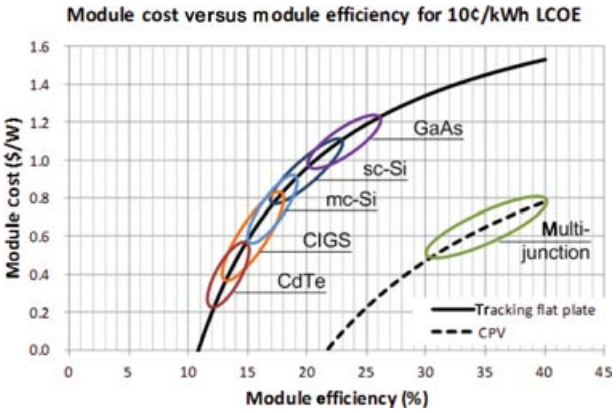

FIGURE 16 | The cost-efficiency ranges for PV modules made of different materials at a target LCOE of 10 ¢/kWh, for tracking flat plate and CPV systems.

tracking flat plate, and CPV. The detailed parameters for fixed and tracking flat plate configurations are depicted in Ref 24. Tracking flat plate systems incorporate extra BOS cost of \$74/m^2 due to introduction of the 1-axis trackers.[24] For CPV, extra BOS cost was considered for high accuracy trackers. \$320/m^2 CPV tracker cost has been derived based on literature published in 2010.[95] However, recent data show a 50% cut of the tracker cost.[96] Therefore, \$160/m^2 is assumed in the calculation here. LCOE values are calculated by running SAM; CPV configuration only considers DNI as the usable irradiation and the temperature coefficients are for III–V materials.

All the three curves in Figure 15 demonstrate the same tendency: as module efficiency increases, module cost is allowed to be higher for the same target LCOE because the fixed BOS expenses can be offset by more energy created. A comparison between tracking and fixed flat plate configurations shows that the allowed module cost in tracking systems has a greater sensitivity to module efficiency. This can be explained by the fact that the extra cost of trackers increases the ratio of the fixed BOS expenses to the total system cost.

A comparison between CPV and flat plate (fixed or tracking) shows that for the same target LCOE, module cost for CPV needs to be much lower than that for flat plate. Two apparent reasons are: (1) only the direct beam can be utilized by CPV, whereas flat plate can use both direct and diffuse light; and (2) CPV needs more expensive trackers. Compared with flat plate systems adopting single-junction solar cells, CPV systems apply multi-junction cells and extra energy loss is caused by current mismatch among subcells under real operating conditions. Here, we estimate this loss to be 10% in long-term operation. Another loss for CPV resides in its high sensitivity to tracking error. Here, we estimate this loss to be 5% in long-term operation. These two factors are incorporated in LCOE calculation; they are not used to modify module efficiency shown in the *x*-axis in Figure 15.

Returning to the PV technologies discussed in the previous section, instead of predicting specific module efficiencies and costs, we specify a range for each type on the module cost versus efficiency curves. For future PV modules, the efficiencies range from the current achievements on the best commercial products. For thin film GaAs, the modules are still under development and no commercial products are available at this moment. Assuming commercial modules in the near future can achieve 85% of the current laboratory module record, we set the starting point of module efficiency range for GaAs at 20%. The end point is defined by multiplying the laboratory cell efficiencies by a constant of 91.6%, which is the highest ratio between laboratory module efficiencies and laboratory cell efficiencies observed on cs-Si. For instance, the upper limit of module efficiency for thin film GaAs is defined at 25.9%. The ranges for different PV modules are depicted in Figure 16. The curve for fixed flat plate is not shown in Figure 16, considering that tracking flat plate is the superior configuration.

The curves in Figure 16 are based on current BOS expenses. However, as R&D efforts and expanded market capability drive down module cost, BOS expenses are also expected to experience the same tendency.[23] Assuming a 30% decrease on BOS expenses without changes of component ratios, we develop another group of curves and ranges, as shown in Figure 17.

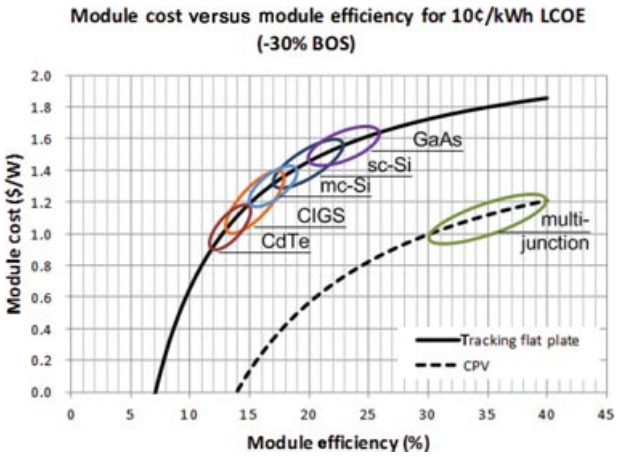

FIGURE 17 | The cost-efficiency ranges for PV modules made of different materials at a target LCOE of 10¢/kWh, for tracking flat plate and CPV systems, and under the assumption of 30% BOS cost reduction.

Figure 17 provides a general picture for future high efficiency and low cost PV modules. This picture is expected to be realized under efforts from multiple levels and sources: R&D activities create new opportunities for higher efficiency and/or lower cost PV components; the industry adopts new approaches and transfers them from laboratory to high volume production; market scaling reduces the unit cost of the components; and the government provides policy support before the grid parity is finally achieved. PV has started its journey to becoming a major electricity source, and continuous efforts focusing on high efficiency will accelerate the progress.

NOTES

[a]When this article was prepared, the installation data for the fourth quarter of 2011 was not available yet; only data for the first three quarters are included here.

[b]Here, we are discussing the real money value instead of the nominal value. Also, the time value of money is not incorporated into the first-order approximation.

[c]For comparison, the 2012 total budget request by Department of Energy (DOE) is $29.5 billion.[18]

[d]Here, we are discussing the real LCOE value, instead of the nominal LCOE value that includes inflation.

[e]This model is currently renamed as the System Advisor Model, and it incorporates analysis function for other renewable energy systems besides solar.

[f]More details about other performance parameters, financing, and incentives can be found in Ref 24.

[g]These LCOE values incorporate 8% state tax and 35% federal tax, and can be compared with market electricity price.

[h]The calculation details and results of LCOE without considering the sales taxes can be found in Ref 24.

[i]The efficiency values in the most recent solar cell efficiency table (Version 39; Ref 27) are not exactly the same as the values in the original publications. This is because the standard spectrum used for calibration has been changed.

[j]Single-crystalline and multi-crystalline together occupy more than 85% of the whole PV market.[2]

[k]Different dividing lines for the concentration categories exist. Here, we give general discussions instead of strict standards about how to define concentration ranges.

[l]The first two issues are also present in reflective concentrator systems. The chromatic aberration results in an expansion of the focused spot, and it is caused by wavelength-dependent refraction index of a Fresnel lens, which is not a problem for reflective concentrators.

[m]Hourly irradiation data from Typical Meteorological Year 2 (TMY2) is used for calculation.

[n]For CPV, module cost in units of $/W refers to irradiation condition of 850W/m^2.

REFERENCES

1. Perlin, J. *The Sillicon Solar Cell Turns 50. NREL Report No. BR-520-33947;* August 2004. Available at: http://www.nrel.gov/docs/fy04osti/33947.pdf. (Accessed June 15, 2012).
2. Earth Policy Institute from European Photovoltaic Industry Association (EPIA), Global Market Outlook for Photovoltaics Until 2013 (Brussels: April 2009), p. 3; EPIA, Global Market Outlook for Photovoltaics Until 2015 (Brussels: May 2011), p. 8. Available at: http://www.earth-policy.org/data_center/C23. (Accessed March 24, 2012).
3. EPIA market report 2011. Available at: http://ht.ly/8Jp9M. (Accessed March 24, 2012).
4. IndexMundi. World Electricity Consumption; January 2011. Available at: http://www.indexmundi.com/g/g.aspx?c=xx&v=81. (Accessed June 15, 2012).
5. Ardani K, Margolis R. *2010 Solar Technologies Market Report*. US Department of Energy; 2011.
6. Bolinger M, Wiser R. *Understanding trends in wind turbine prices over the past decade*. Lawrence Berkeley National Laboratory; 2011.

7. International Energy Agency. Trends in photovoltaic applications survey report of selected IEA countries between 1992 and 2010. *Report IEA-PVPS T1-20*; 2011.
8. SEIA, GTM. US solar market insight Report, Q3 2011. *Executive Summary*; 2011.
9. Laherrère JH. *The Hubbert Curve: Its Strength and Weaknesses*. 2000. Available at: http://dieoff.org/page191.htm. (Accessed March 24, 2012).
10. Meyer PS, Yung JW, Ausubel JH. A Primer on logistic growth and substitution: the mathematics of loglet lab software. *Technology Forecasting and Social Change* 1999, 61:247–271.
11. Denholm P, Margolis R. *Very large-scale deployment of grid-connected solar photovoltaics in the United States: challenges and opportunities*. National Renewable Energy Laboratory; 2006.
12. Available at: http://www.eia.gov/electricity/data/state/. (Accessed March 24, 2012).
13. Available at: http://www.eia.gov/forecasts/aeo/er/index.cfm. (Accessed March 24, 2012).
14. Rogers EM. *Diffusion of Innovations*. Glencoe: Free Press; 1962.
15. Byrne J, Kurdgelashvili L. *Chapter 2 of Handbook of Photovoltaic Science and Engineering*. 2nd ed. Chichester, West Sussex, UK: John Wiley & Sons; 2011.
16. Barbose G, Darghouth N, Wiser R, Seel J. *Tracking the sun IV: an historical summary of the installed cost of photovoltaics in the United States from 1998 to 2010*. Lawrence Berkeley National Laboratory; 2011.
17. Zwaan B, Rabl A. Prospects for PV: a learning curve analysis. *Solar Energy* 2003, 74:19–31.
18. Office of Chief Financial Officer. Department of Energy FY 2012 Congressional Budget Request. DOE/CF-0059; 2012.
19. Available at: http://www.nrel.gov/ncpv/images/efficiency_chart.jpg. (Accessed March 24, 2012).
20. Schmieder K, Haughn C, Pulwin Z, Dyer D, Barclay L, Doty M, Ebert C, Barnett A. Analysis of high growth rate MOCVD structures by solar cell device measurements and time-resolved photoluminescence. *37th IEEE Photovoltaic Specialists Conference*; 2011.
21. Short W, Packey D, Holt T. A manual for the economic evaluation of energy efficiency and renewable energy technologies. NREL/TP-462-5173; 1995.
22. Available at: https://sam.nrel.gov/. (Accessed March 24, 2012).
23. Bony L, Doig S, Hart C, Maurer E, Newman S. *Achieving low-cost solar PV: industry workshop recommendations for near-term balance of system cost reductions*. 2010.
24. Wang X, Kurdgelashvili L, Byrne J, Barnett A. The value of module efficiency in lowering the levelized cost of energy of photovoltaic systems. *Renewable and Sustainable Energy Reviews* 2011, 15:4248–4254.
25. Zhao J, Wang A, Green MA, Ferrazza F. Novel 19.8% efficient "honeycomb" textured multicrystalline and 24.4% monocrystalline silicon solar cells. *Appl Phys Lett* 1998, 73:1991–1993.
26. Zhao J, Wang A, Yun F, Zhang G, Roche DM, Wenham SR, Green MA. 20,000 PERL silicon cells for the "1996 world solar challenge" solar car race. *Progr Photovoltaics: Res Appl* 1997, 5:269–276.
27. Green MA, Emery K, Hishikawa Y, Warta W, Dunlop ED. Solar cell efficiency tables (version 39) progress in photovoltaics. *Res Appl* 2012, 20:12–20.
28. Tiedje T, Yablonovitch E, Cody GD, Brooks BG. Limiting efficiency of silicon solar cells. *IEEE Trans Electron Devices* 1984, 31:711–716.
29. Available at: http://en.wikipedia.org/wiki/File:PV_Technology.png. (Accessed March 24, 2012).
30. Schultz O, Glunz SW, Willeke GP. Multicrystalline silicon solar cells exceeding 20% efficiency. *Progr Photovoltaics: Res Appl* 2004, 12:553–558.
31. Saitoh T, Hashigami H, Rein S, Glunz S. Overview of light degradation research on crystalline silicon solar cells. *Progr Photovoltaics: Res Appl* 2000, 8:535–547.
32. Tobías I, Cañizo CD, Alonso J. *Chapter 7 of Handbook of Photovoltaic Science and Engineering*. 2nd ed. Chichester, West Sussex, UK: John Wiley & Sons; 2011.
33. Sopori BL, Deng X, Benner JP, Rohatgi A, Sana P, Estreicher SK, Park YK, Roberson MA. Hydrogen in silicon: a discussion of diffusion and passivation mechanisms. *Solar Energy Mater Solar Cells* 1996, 41/42:159–169.
34. Available at: http://global.sunpowercorp.com/products/solar-panels/. (Accessed March 24, 2012).
35. Verlinden P, Sinton RA, Wickham K, Crane RA, Swanson RM. Backside-contact silicon solar cells with improved efficiency for the '96 world solar challenge. *Proceedings of the 14th EPVSC*; 1997, 96–99.
36. Aberle AG. Surface passivation of crystalline silicon solar cells: a review. progress in photovoltaics. *Res Appl* 2000, 8:473–487.
37. Green M. *Chapter 6 of Silicon Solar Cells: Advanced Principles and Practice*. Centre for Photovoltaic Devices and Systems, University of New South Wales, Sydney; 1995.
38. Henley F, Lamm A, Kang S, Liu Z, Tian L. Direct film transfer (DFT) technology for kerf-free silicon wafering. *Proceedings of the 22nd EU PVSEC*; 2008, 1090–1093.
39. Hopman S, Fell A, Mayer K, Mesec M, Willeke GP, Kray D. First results of wafering with laser chemical processing. *Proceedings of the 22nd EU PVSEC*; 2008, 1131–1135.
40. Brendel R. A novel process for ultrathin monocrystalline silicon solar cells on glass. *Proceedings of 14th EU PVSEC*; 1997, 1354–1357.

41. Petermann JH, Zielke D, Schmidt J, Haase F, Rojas EG, Brendel R. 19%-efficient and 43 μm-thick crystalline Si solar cell from layer transfer using porous silicon. *Progr Photovoltaics: Res Appl* 2012, 20:1–5.
42. Shafarman W, Siebentritt S, Stolt L. *Chapter 13 of Handbook of Photovoltaic Science and Engineering*. 2nd ed. Chichester, West Sussex, UK: John Wiley & Sons; 2011.
43. Repins I, Contreras MA, Egaas B, DeHart C, Scharf J, Perkins CL, To B, Noufi R. 19.9% Efficient ZnO/CdS/CuInGaSe^2 solar cell with 81.2% fill factor. *Progr Photovoltaics: Res Appl* 2008, 16:235–239.
44. Hedstrom J, Ohlsen H, Bodegard M, Kylner A, Stolt L, Hariskos D, Ruckh M, Schock HW. ZnO/CdS/Cu(In,Ga)Se_2 thin film solar cells with improved performance. *Proceedings of the 23rd IEEE PVSC* 1993, 364–371.
45. Kronik L, Cahen D, Schock H. Effects of sodium on polycrystalline Cu(In,Ga)Se_2 and its solar cell performance. *Adv Mater* 1998, 10: 31–36.
46. Niles D, Al-Jassim M, Ramanathan K. Direct observation of Na and O impurities at grain surfaces of CuInSe2 thin films. *J Vacuum Sci Technol A* 1999, 17:291–296.
47. Boyd D, Thompson D. *Kirk-Othmer Encyclopaedia of Chemical Technology*, 3rd ed. New York, USA: John Wiley & Sons, Inc. 1980, 11:807–880.
48. Kessler F, Herrmann D, Powalla M. Approaches to flexible CIGS thin-film solar cells. *Thin Solid Films* 2005, 480/481:491–498.
49. Yan Yanfa, Jiang C-S, Noufi R, Wei Su-Huai, Moutinho HR, Al-Jassim MM. Electrically benign behavior of grain boundaries in polycrystalline $CuInSe_2$ films. *Phys Rev Lett* 2007, 99:235504.
50. Hetzer MJ, Strzhemechny YM, Gao M, Contreras MA, Zunger A, Brillson LJ. Direct observation of copper depletion and potential changes at copper indium gallium diselenide grain boundaries. *Appl Phys Lett* 2005, 86:162105.
51. Lei C, Li CM, Rockett A, Robertson IM. Grain boundary compositions in Cu(InGa)Se_2. *J Appl Phys* 2007, 101:024909.
52. Yan Y, Noufi R, Al-Jassim M. Grain-boundary physics in polycrystalline $CuInSe_2$ revisited: experiment and theory. *Phys Rev Lett* 2006, 96:205501.
53. Seto J. The electrical properties of polycrystalline silicon films. *J Appl Phys* 1975, 46:5247.
54. Siebentritt S, Schuler S. Defects and transport in the wide gap chalcopyrite $CuGaSe_2$. *J Phys Chem Solids* 2003, 64:1621–1626.
55. Available at: http://en.wikipedia.org/wiki/First_Solar. (Accessed March 24, 2012).
56. Available at: http://www.firstsolar.com/~/media/WWW/Files/Downloads/PDF/Datasheet_s3_NA.ashx. (Accessed March 24, 2012).
57. McCandless BE, Sites JR. *Chapter 14 of Handbook of Photovoltaic Science and Engineering*. 2nd ed. Chichester, West Sussex, UK: John Wiley & Sons; 2011.
58. Wei S, Zhang X. Chemical trends of defect formation and doping limit in II-VI semiconductors: the case of CdTe. *Phys Rev B* 2002, 66:155211.
59. Castaldini A, Cavallini A, Fraboni B. Deep energy levels in CdTe and CdZnTe. *J Appl Phys* 1998, 83:2121–2126.
60. Stollwerck G, Sites J. Analysis of CdTe back contact barriers. *Proceedings of the 13th EU PVSEC*; 1995, 2020–2022.
61. Kayes BM, Nie H, Twist R, Spruytte SG, Reinhardt F, Kizilyalli IC, Higashi GS. 27.6% Conversion efficiency, a new record for single-junction solar cells under 1 sun illumination. *Proceedings of 37th IEEE PVSC*; 2011.
62. Available at: http://en.wikipedia.org/wiki/Concentrated_photovoltaics. (Accessed March 24, 2012).
63. Torrey E, Ruden P, Cohen P. Performance of a split-spectrum photovoltaic device operating under time-varying spectral conditions. *J Appl Phys* 2011, 109:074909.
64. Geisz JF, Friedman DJ, Ward JS, Duda A, Olavarria WJ, Moriarty TE, Kiehl JT, Romero MJ, Norman AG, Jones KM. 40.8% Efficient inverted triple-junction solar cell with two independently metamorphic junctions. *Appl Phys Lett* 2008, 93:123505.
65. Geisz JF, Kurtz S, Wanlass MW, Ward JS, Duda A, Friedman DJ, Olson JM, McMahon WE, Moriarty TE, Kiehl JT. High-efficiency GaInP/GaAs/InGaAs triple junction solar cells grown inverted with a metamorphic bottom junction. *Appl Phys Lett* 2007, 91:023502.
66. Friedman DJ, Olson JM, Kurtz S. *Chapter 8 of Handbook of Photovoltaic Science and Engineering*. 2nd ed. Chichester, West Sussex, UK: John Wiley & Sons; 2011.
67. Available at: http://rredc.nrel.gov/solar/spectra/am1.5/ASTMG173/ASTMG173.html. (Accessed March 24, 2012).
68. Brown A, Green M. Detailed balance limit for the series constrained two terminal tandem solar cell. *Physica E* 2002, 14:96–100.
69. Shockley W, Queisser H. Detailed Balance limit of efficiency of P-N junction solar cells. *J Appl Phys* 1961, 32:510.
70. Henry C. Limiting efficiencies of ideal single and multiple energy gap terrestrial solar cells. *J Appl Phys* 1980, 51:4494.
71. Wang X, Barnett A. Value of module efficiency in real operating conditions for low energy cost PV systems. *37th IEEE Photovoltaic Specialists Conference*; 2011.
72. Wang X, Barnett A. The effect of spectrum variation on the energy production of triple-junction solar cells. *J Photovoltaics* (in review).

73. Muller M, Marion B, Kurtz S, Rodriguez J. An investigation into spectral parameters as they impact CPV module performance. *Proceedings of the 6th International Conference on Concentrating Photovoltaic Systems* 2010, 307–311.
74. Peharz G, Siefer G, Araki K, Bett AW. Spectrometric outdoor characterization of CPV modules using isotype monitor cells. *Proceedings of the 33rd IEEE PVSC* 2008, 1–5.
75. Philipps S, Peharz G, Hoheisel R, Hornung T, Alabbadi NM, Dimroth F, Bett AW. Energy harvesting efficiency of III-V triple-junction concentrator solar cells under realistic spectral conditions. *Solar Energy Materials Solar Cells* 2010, 94:869–877.
76. Chan N, Young T, Brindley H, Chaudhuri B, Ekins-Daukes NJ. Variation in spectral irradiance and the consequences for multi-junction concentrator photovoltaic systems. *Proceedings of the 35th IEEE PVSC* 2010, 003008–003012.
77. Kinsey G, Nayak A, Liu M, Garboushian V. Increasing power and energy in Amonix CPV solar power plants. *Journal of Photovoltaics* 2011, 1:213–218.
78. Dobbin A, Georghiou G, Lumb M, Norton M, Tibbits T. Energy Harvest Predictions for a Spectrally Tuned Multiple Quantum Well. *7th International CPV Conference*; 2011.
79. Dimroth F, Baur C, Bett AW, Meusel M, Strobl G. 3–6 Junction photovoltaic cells for space and terrestrial concentrator applications. *Proceedings of the 31st IEEE PVSC* 2005, 525–529.
80. Torrey E, Krohn J, Ruden P, Cohen P. Efficiency of a lateral engineered architecture for photovoltaics. *Proceedings of the 35th IEEE PVSC* 2010, 002978–002983.
81. Vincenzi D, Busato A, Stefancich M, Martinelli G. Concentrating PV system based on spectral separation of solar radiation. *Physica Status Solidi (A)* 2009, 206:375–378.
82. Barnett A, Wang X, Waite N, Murcia P, Honsberg C, Kirkpatrick D, Laubacher D, Kiamilev F, Goossen K, Wanlass M, et al. Initial test bed for very high efficiency solar cells. *Proceedings of the 33rd IEEE PVSC* 2008, 1–7.
83. Wang X, , Waite N, Murcia P, Emery K, Steiner M, Kiamilev F, Goossen K, Honsberg C, Barnett A. Lateral spectrum splitting concentrator photovoltaics: direct measurement of component and submodule efficiency. *Progr Photovoltaics: Res Appl* 2012, 20:149–165.
84. McCambridge J, Steiner M, Unger B, Emery K, Christensen E, Wanlass M, Gray A, Takacs L, Buelow R, McCollumT, et al. Compact spectrum splitting photovoltaic module with high efficiency. *Progr Photovoltaics: Res Appl* 2011, 19:352–360.
85. Lucovsky G. Photoeffects in nonuniformly irradiated P-N junctions. *J Appl Phys* 1960, 31:1088.
86. Kurtz S. Estimating and controlling chromatic aberration losses for two-junction, two-terminal devices in refractive concentrator systems. *Proceedings of the 25th IEEE PVSC* 1996, 361–364.
87. Ota Y, Nishioka K. Three-dimensional simulation of concentrator photovoltaic modules using raytrace and equivalent circuit simulators. *Solar Energy* 2012, 86:476–481.
88. Sala G, Antón I. *Chapter 10 of Handbook of Photovoltaic Science and Engineering*. 2nd ed. Chichester, West Sussex, UK: John Wiley & Sons; 2011.
89. Available at: http://www.lapptannehill.com/suppliers/literature/3m/Factors.pdf. (Accessed March 24, 2012).
90. Available at: http://www.semprius.com/news_pr.php. (Accessed March 24, 2012).
91. Bower CA, Menard E, Garrou PE. Transfer printing: an approach for massively parallel assembly of microscale devices. *Proceedings of the 58th ECTC* 2008, 1105–1109.
92. Burroughs S, Conner R, Furman B, Menard E, Gray A, Meitl M, Bonafede S, Kneeburg D, Ghosal K, Bukovnik R, Wagner W, Seel S. A new approach for a low cost CPV module design utilizing micro-transfer printing technology. *Proceedings of the 6th International Conference on Concentrating Photovoltaic Systems* 2010, 163–166.
93. Ebert C, Parekh A, Pulwin Z, Zhang W, Lee D, Byrnes D. Fast growth rate GaAs and InGaP for MOCVD grown triple junction solar cells. *Proceedings of the 35th IEEE PVSC* 2010, 002007–002011.
94. Furman B, Menard E, Gray A, Meitl M, Bonafede S, Kneeburg D, Ghosal K, Bukovnik R, Wagner W, Gabriel J, et al. A high concentration photovoltaic module utilizing micro-transfer printing and surface mount technology. *Proceedings of the 35th IEEE PVSC* 2010, 000475–000480.
95. Seshan C. CPV: not just for hot deserts. *Proceedings of the 35th IEEE PVSC* 2010, 003075–003080.
96. Available at: http://www.alibaba.com/product-gs/450240568/CPV_sun_tracker_solar_system.html. (Accessed March 24, 2012).

